A Numerical Examination of the Castro-Mahecha Supersymmetric Model of the Riemann Zeros

Paul B. Slater*

ISBER, University of California,

Santa Barbara, CA 93106

(Dated: May 22, 2006)

Abstract

The unknown parameters of the recently-proposed (*Int J. Geom. Meth. Mod. Phys.* **1**, 751 [2004]) Castro-Mahecha model of the imaginary parts (λ_j) of the nontrivial Riemann zeros are the phases (α_k) and the frequency parameter (γ) of the Weierstrass function of *fractal* dimension $D = \frac{3}{2}$ and the turning points (x_j) of the *supersymmetric* potential-squared $\Phi^2(x)$ — which incorporates the *smooth* Wu-Sprung potential (*Phys. Rev.* E **48**, 2595 [1993]), giving the *average* level density of the Riemann zeros. We conduct numerical investigations to estimate/determine these parameters — as well as a parameter (σ) we introduce to *scale* the fractal contribution. Our primary analyses involve two sets of *coupled* equations: one set being of the form $\Phi^2(x_j) = \lambda_j$, and the other set corresponding to the fractal extension — according to an *ansatz* of Castro and Mahecha – of the Comtet-Bandrauk-Campbell (CBC) quasi-classical quantization conditions for good supersymmetry, $\frac{2}{\Gamma(D/2)} \int_{-x_j}^{x_j} \frac{[\lambda_j - \Phi^2(x')]^{1/2}}{(x_j - x')^{1-D/2}} dx' = j\pi$. Our analyses suggest the possibility strongly that γ converges to its theoretical lower bound of 1, and the possibility that all the phases (α_k) should be set to zero. We also uncover interesting formulas for certain fractal turning points.

PACS numbers: Valid PACS 02.10.De, 03.65.Sq, 05.45.Df, 11.30.Pb

Keywords: Riemann zeros, Wu-Sprung potential, Weierstrass fractal function, supersymmetry, Castro-Mahecha model, Comtet-Bandrauk-Campbell (CBC) formula, turning points, Riemann Hypothesis, simultaneous nonlinear equations, Brownian motion

*Electronic address: slater@kitp.ucsb.edu

I. INTRODUCTION

The precise nature of the *zeros* of the Riemann zeta function is of paramount mathematical [1], as well as physical interest [2]. Of course, perhaps the most famous, not yet fully resolved, mathematical conjecture (the Riemann Hypothesis [3]) is that *all* the non-trivial zeros $(\eta_j + i\lambda_j)$ — the trivial zeros simply equalling $-2j$, $j = 1, 2, 3, \ldots$ — have real components $\eta_j = \frac{1}{2}$.

Castro and Mahecha [4] recently proposed a *supersymmetric* implementation of the Wu-Sprung model [5] of the λ_j's, employing a Weierstrass (continuous and nowhere differentiable) function [6] for the *fractal* structure of dimension $D = \frac{3}{2}$ that Wu and Sprung had found for their local one-dimensional potential (V) (cf. [7, 8]). The Wu-Sprung potential V — which generates the smooth *average* level density obeyed by the Riemann zeros — satisfied *Abel's integral equation* [5, eq. (6)], and was written implicitly as [5, eq. (7)],

$$x = \frac{1}{\pi}\Big(\sqrt{V - V_0}\ln\frac{V_0}{2\pi e^2} + \sqrt{V}\ln\frac{\sqrt{V} + \sqrt{V - V_0}}{\sqrt{V} - \sqrt{V - V_0}}\Big). \tag{1}$$

Here $V_0 = 3.10073\pi \approx 9.74123$.

The Weierstrass fractal function employed by Castro and Mahecha [4, eq. (81)],

$$W(x, \gamma, D, \alpha_k) = \Sigma_{k=0}^{\infty}\frac{1 - e^{ix\gamma^k}}{\gamma^{k(2-D)}}e^{2\pi i\alpha_k}, \tag{2}$$

has both an unknown (countably) infinite set of phases $2\pi\alpha_k$ and an unknown parameter γ, which determines the frequencies γ^k. Further, D is the fractal dimension, which Castro and Mahecha — following the box-counting argument of Wu and Sprung [5] (cf. [9]) — took to be $\frac{3}{2}$. (Castro and Mahecha also noted [4, sec. 6] that this choice of $D = \frac{3}{2}$ does, appealingly, yield [the omnipresent] $\frac{1}{f}$ noise.) The variable x parameterizes the *inverted* Wu-Sprung potential $V_{WS}(x)$, which in accordance with the supersymmetric requirement that the energy be zero in the ground state, was translated to be zero at $x = 0$.

Rather than *directly* addressing the formidable problem "of factoring the ordinary Schrödinger equation studied by Wu-Sprung", Castro and Mahecha (CM) postulated the model [4, eq. (82)],

$$\Phi^2(x) = V_{WS}(x) + \frac{1}{2}[W(x, D, \gamma, \alpha_k) + W(-x, D, \gamma, \alpha_k) + c.c.] + \phi_0, \tag{3}$$

with

$$\Phi^2(x_j) = \lambda_j. \tag{4}$$

(*c.c.* denotes complex conjugation.) The additive constant $\phi_0 = -V_0$ is chosen so that, in accordance with supersymmetric principles, $\Phi^2(0) = 0$. The "turning points" x_j (where the potential energy is equal to the total energy), along with the phases α_k and the parameter γ, are the unknown (countably infinite) parameters of the CM model, which we hope here to estimate/determine, by satisfying the equations (3), *simultaneously* with the *quantization* conditions [4, eq. (87)],

$$I_j(x_j, \lambda_j) \equiv 2\frac{1}{\Gamma(\beta)} \int_{-x_j}^{x_j} \frac{[\lambda_j - \Phi^2(x')]^{1/2}}{(x_j - x')^{1-\beta}} dx' = j\pi. \tag{5}$$

Castro and Mahecha proposed (cf. [10, eq. (36)]) that these relations would constitute the *fractal* extension of the fermionic phase path integral approximation (the CBC [Comtet-Bandrauk-Campbell] formula (cf. [11, eq. (1)] [5, eq. (5)])) — the supersymmetric counterpart of the well-known *WKB* quantization rule [11, eq. (2)]. Here $\beta = \frac{D}{2} = \frac{3}{4}$ and j runs over the positive integers.

The Castro-Mahecha model (3) was cast in a fractal supersymmetric quantum-mechanical (SUSY-QM) setting, in an effort to implement the *Hilbert-Polya* proposal [12] to prove the Riemann Hypothesis, under which an Hermitian operator, hypothetically, can be found to reproduce the λ_j's as its *spectrum*. It had appeared to CM quite difficult to directly solve the SUSY Schrödinger equation [4, eq. (84)],

$$(\mathcal{D}^{(\beta)} + \Phi)(-\mathcal{D}^{(\beta)} + \Phi)\psi_j^{(+)}(x) = \lambda_j \psi_j^{(+)}(x), \tag{6}$$

where $\hbar = 2m = 1$, $\lambda_j^{(+)} = \lambda_j^{(-)}$, the $\psi_j^{(+)}$ are eigenfunctions, and the *fractional* derivative

$$\mathcal{D}^{(\beta)} F(t) = \frac{1}{\Gamma(1-\beta)} \frac{d}{dt} \int_{-\infty}^{t} \frac{F(t')}{(t-t')^{\beta}} dt', \tag{7}$$

is intended (cf. [10]). (M. Trott suggested that one might *directly* pursue the solution of this system, most effectively, using a *Grünwald-Letnikov* discrete approximation [13].) CM, therefore, had recourse to the CBC formula (5) as an *approximation* to the implementation of the quantum *inverse scattering* method, which would yield the potential Φ. Given an exact potential, one could construct the SUSY Schrödinger equation, giving the λ_j's for its eigenvalues. This would realize — CM claimed — the Hilbert-Polya proposal to prove the Riemann Hypothesis.

CM reasoned that if the potential energy has the shape of a fractal curve, then it is very natural to assume that the kinetic energy operator should be a fractal; namely it should be expressed in terms of *fractal* derivatives.

In sec. II, we begin our numerical analyses by studying the solutions to (3). Then, in sec. III, we extend the analyses to include (simultaneously) the two sets of equations (3) and (5). The *fractal* Wu-Sprung potential V is examined in sec. IV, in particular its turning points, for a number of which interesting formulas are obtained. In sec. V, we expand the CM model to include a certain scaling factor. A discussion of our analyses is contained in sec. VI. We also include an Appendix outlining recent work of D. Dominici concerning the *inversion* of the Wu-Sprung potential [14].

II. PRELIMINARY ANALYSES

A. Turning points $x_j^{(1)}$ — for smooth potential — held fixed

Our initial numerical analyses of the CM model consisted of, for various integral cut-offs m on the running index k in the Weierstrass fractal function summation (2), finding an optimizing set of α_k's, while keeping the x_j's *fixed* and equal to (n of) the turning points for the translated inverted *smooth* Wu-Sprung potential, that is, those $x_j^{(1)}$'s for which (cf. (3)),

$$V_{WS}(x_j^{(1)}) + \phi_0 = \lambda_j. \tag{8}$$

The set of estimated α_k's and γ would be chosen, so as to minimize the sum of squared deviations — since it did not appear possible to achieve complete equality — between the LHS (left-hand side) and RHS of (8). Computationally-speaking we employed the NMinimize command of Mathematica, using the "DifferentialEvolution" and "InitialPoints" options, and for the initial points only *increasing* sets of values for the α_k's, in order to reduce search times. Also, the *necessary* inversion of the Wu-Sprung potential (1) — in order to obtain $V_{WS}(x)$ — was performed using the Interpolation command of Mathematica (cf. Appendix).

We, first, found certain evidence, at least in this initial context, that suggested taking $\gamma = 3 = 2D$. (In [4], CM wrote that "it would be intriguing to see if $\gamma = 1 + \phi \approx 1.618$, the inverse of the golden mean, since the golden mean appears in the theory of quantum noise related to the Riemann Hypothesis" (cf. [6, p. 481]).

Initially, we tried the case $n = 100, m = 15$, insisting that the phases be ordered from lowest to highest. Our results were encouraging, and we proceeded to successively higher integral values of m, reaching $m = 100$. (We make the obvious comment that here the

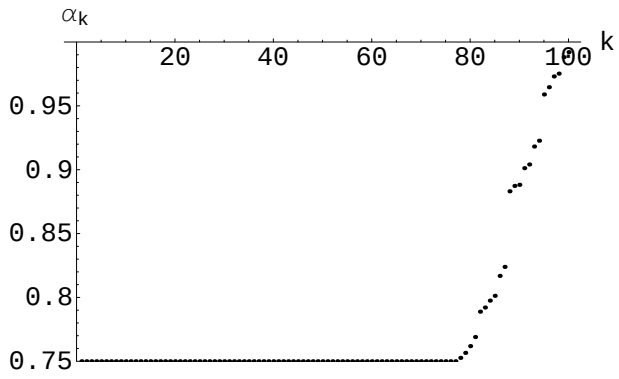

FIG. 1: The one hundred ordered phases (divided by 2π) of the Weierstrass fractal function (2) obtained by minimizing the sum-of-squares deviation from the imaginary parts of the first one hundred nontrivial Riemann zeros of the Castro-Mahecha supersymmetric model (3)

number m of unknowns $[\alpha_k]$ *equals* the number of [nonlinear] equations.) For that case, the best fit to the first 100 λ_j's yielded a *remarkably* small sum-of-squares deviations of $2.68927 \cdot 10^{-14}$. The first *seventy-seven* of the hundred ordered phases (that is, $2\pi\alpha_k, k = 1, \ldots, 70$) were *all* equal to $\frac{3\pi}{2} = 2\pi\beta$ to, typically, seven decimal places (Fig. 1). When we inserted the turning points ($x_j^{(1)}$) derived from the (smooth) inverted Wu-Sprung potential for the bounds of integration — that is, those satisfying (8) — into the fractal CBC formula (5), we found that these quantization relations were clearly *not* fully met. (In general, the CBC quantization conditions appear to hold for a number of "shape-invariant" potentials [11] (cf. [15]).) In Fig. 2, we plot the (CBC) *ratio* of the computed value of the real part of the LHS of (5) to its RHS (that is, $j\pi$). We see that for the lower values of j, the LHS's *exceed* $j\pi$, while for the higher values, they are less than $j\pi$ — all in an apparently smooth monotonically decreasing manner.

We, then, were able to extend our computer analyses to the case $n = m = 200$, with very analogous results (Fig. 3). (The sum of squared deviations was quite small, as in the $n = m = 100$ analysis, $3.48792 \cdot 10^{-14}$.) Most of the estimated values of α_k were once again $\frac{3}{4}$ to high precision, this time for $k = 1, \ldots, 144$. In Fig. 4 we present the analogue of Fig. 2 for the $n = m = 200$ case.

In regard to the phases of the Weierstrass fractal function, Castro and Mahecha [16, sec. 5] had written that it "is warranted to see if the statistical distribution of these phases α_k has any bearing to random matrix theory (the circular unitary random matrix ensemble) and

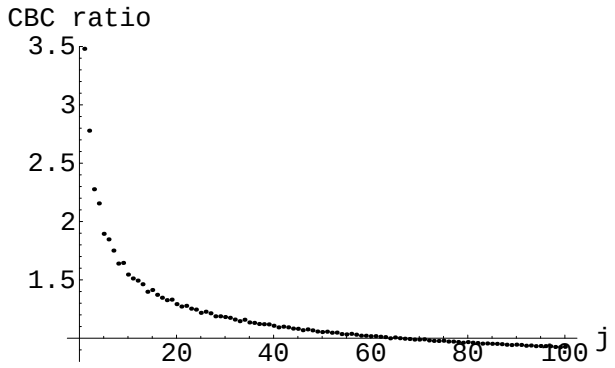

FIG. 2: Ratios of the (real parts of the) computed values of the left-hand side of the fractal CBC quantization conditions (5) — based on the (fixed) turning points, those x_j for which $\lambda_j = V_{WS}(x_j)$, of the *smooth* inverted (translated) Wu-Sprung potential and the scaled phases shown in Fig. 1 — to the right-hand side of (5) (that is, $j\pi$). The ratios would all be unity if the conditions were fully satisfied.

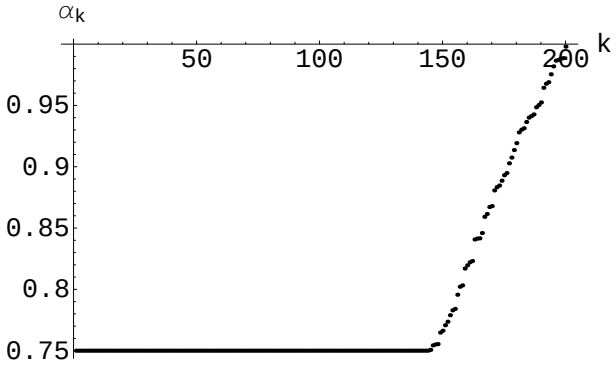

FIG. 3: The *two* hundred ordered phases (divided by 2π) of the Weierstrass fractal function (2) obtained by minimizing the sum-of-squares deviation from the imaginary parts of the first two hundred nontrivial Riemann zeros of the Castro-Mahecha supersymmetric model (3)

the recent studies of quantum phase-locking, entanglement, Ramanujan sums and cyclotomy studied by [16]".

When we proceeded to the still higher-order case $n = 300, m = 300$, we found superficially, at least, different types of results. In six different runs (using different random seeds) of our Mathematica program, we obtained sum-of-squares deviations no greater than $1.79962 \cdot 10^{-13}$, all six yielding essentially the same-looking plot. The smallest sum-of-squares was $1.62071 \cdot 10^{-13}$, corresponding to Fig. 5. The first seventy-four scaled phases (α_k) were

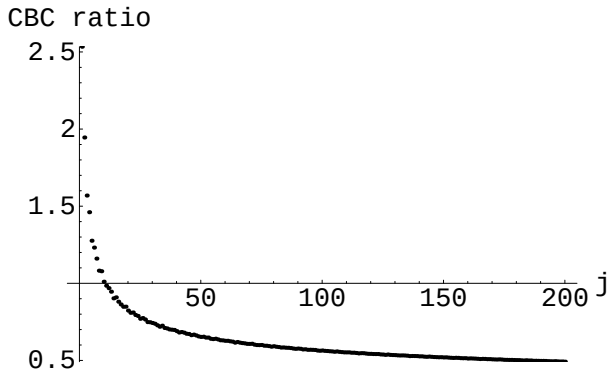

FIG. 4: Ratios, for the case $n = 200$, of the (real parts of the) computed values of the left-hand side of the fractal CBC quantization conditions (5) to the right-hand side of (5) (that is, $j\pi$). The ratios would all be unity if the conditions were fully satisfied.

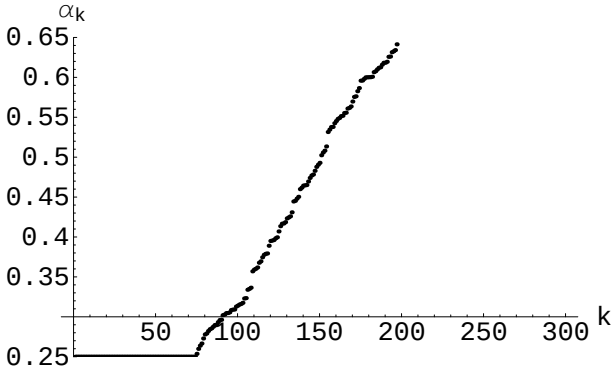

FIG. 5: The *three* hundred ordered phases (divided by 2π) of the Weierstrass fractal function (2) obtained by minimizing the sum-of-squares deviation from the imaginary parts of the first three hundred nontrivial Riemann zeros of the Castro-Mahecha supersymmetric model (3)

all equal to $\frac{1}{4}$ (rather than $\frac{3}{4}$, as previously) to high accuracy. Let us note, in any case though, that for *either* $\alpha_k = \frac{1}{4}$ or $\frac{3}{4}$, the factors $e^{2\pi i \alpha_k}$ in the expansion (2) of the Weierstrass fractal function have *zero* real part.

B. Comment

What it appeared, in retrospect, we had actually principally accomplished above (Figs. 1, 3, 5) was to find sets of phases ($2\pi\alpha_k$) for various n (100, 200 and 300), such that the real part of the Weierstrass fractal function (2) is very close to zero — as revealed by plots —

for *any* x (or $\gamma > 1$), be it a turning point or not. So, these results immediately pertain to the Weierstrass fractal function and not the Riemann zeros themselves. Nevertheless, our estimated phases (α_k's) can be employed as the *first* step of an *iterative* procedure — as discussed in the next section.

Since the Castro-Mahecha supersymmetric model of the Riemann zeros requires the *simultaneous* obtaining/fitting of phases (α_k's), the parameter γ, and turning points (x_j's), we turn to this problem now.

III. *JOINT* ESTIMATION OF PHASES (α_k) AND TURNING POINTS (x_j)

A. Iterative approach

1. $n = m = 100$ *analyses*

We would like now to regard the *two* sets of equations (3) — the *one* set we have tried to satisfy in the above analyses — *and* (5) as a *coupled* system and attempt to *simultaneously* solve for the phases (α_k) *and* turning points (x_j) (still holding $\gamma = 3$). In this context, we again considered the case $n = 100, m = 100$, and took the solution portrayed in Fig. 1 as the first step of an *iterative* procedure. Using this set of $\alpha_k^{(1)}$'s, we searched for a *new* set of turning points ($x_j^{(2)}, j = 1, \ldots, 100$), such that the CBC quantization conditions (5) would *all* be exactly (up to our numerical accuracy) satisfied. Then, with this revised set of x_j's, we hoped to find anew the set of $\alpha_k^{(2)}$'s satisfying (3). By reiterating this two-step procedure a sufficiently large number of times, we anticipated possibly arriving at a *final* set of $\alpha_k^{(N)}$'s and $x_j^{(N)}$'s *simultaneously* satisfying (3) and (5) (cf. [17]). A test for convergence to such a final solution would be that the two sets of parameters would only change negligibly upon further iterations. [33]

At the very beginning of the iterative procedure we have just outlined, we sought to obtain a (hypothetical, second) set of one hundred turning points ($x_j^{(2)}$), which would render the CBC quantization conditions (5) *completely* satisfied when the first set of phases ($2\pi\alpha_k^{(1)}$) — those depicted (in their scaled form) in Fig. 1 — were employed. However, this proved to be not totally doable. For example, for the original value of $x_{100}^{(1)} = 15.315$, the corresponding CBC ratio was 0.926293. But when we tried to adjust $x_{100}^{(1)}$ to increase this ratio closer to the ideal value of 1, we were only able to obtain a *slight* improvement by going to $x_{100}^{(2)} = 14.3452$,

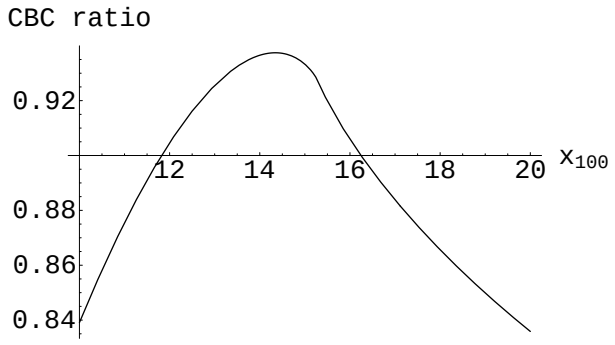

FIG. 6: CBC ratio — incorporating the phases shown in Fig. 1 — as a function of the hundreth turning point (x_{100}). The original value of $x_{100}^{(1)}$, giving a ratio of 0.926293, was 15.315. This can be (only) slightly improved to 0.937452, by choosing $x_{100}^{(2)} = 14.3452$.

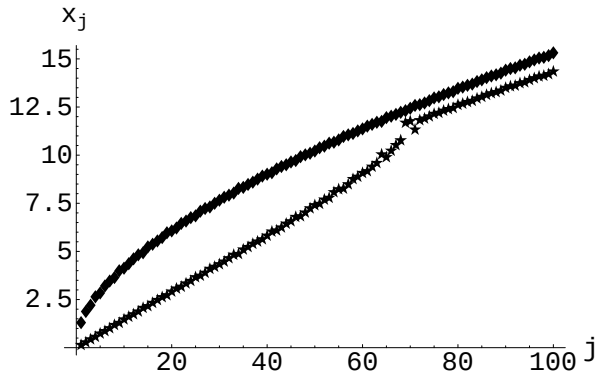

FIG. 7: The original 100 turning points ($x_j^{(1)}$), forming the higher/dominant line, and the 100 adjusted/revised turning points ($x_j^{(2)}$) that yield CBC ratios optimally closer to *unity* — *given* the phases shown in Fig. 1

for which the ratio was 0.937452. We show this phenomenon in Fig. 6.

In *all* one hundred cases, when we sought to drive the CBC ratios closer to unity, the new turning points chosen, $x_j^{(2)}$, were *smaller* than the originals $x_j^{(1)}$ (Fig. 7). (There is some anomalous behavior apparent, in that $x_{71}^{(2)} < x_{70}^{(2)}$.) For the first seventy-one cases, the new turning points ($x_j^{(2)}$) do yield the desired CBC ratio of 1 (Fig. 8). (We have not been able to obtain a revised set of $\alpha_k^{(2)}$'s based on the 100 $x_j^{(2)}$'s to *closely* satisfy (3), as we had with the 100 $x_j^{(1)}$'s.) When the *revised* set of turning points $x_j^{(2)}$ was employed, along with the *original* set of phases $\alpha_k^{(1)}$'s (Fig. 1), instead of highly accurate predictions of the λ_j's, we obtained signficant discrepancies. (The sum-of-squares measure of fit to (3) jumped enormously from

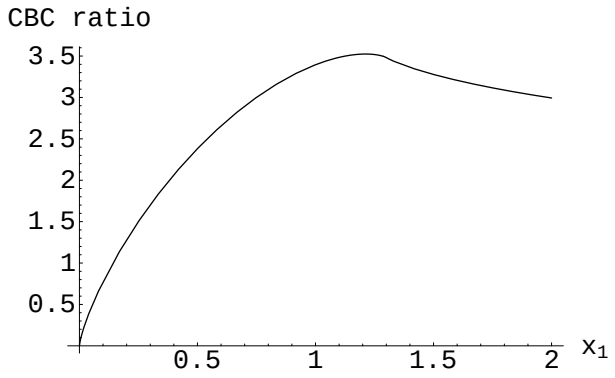

FIG. 8: CBC ratio as a function of the first turning point ($x_1^{(2)}$). The value of $x_1^{(1)}$, which gave (Fig. 2) a ratio of 3.48049, was 1.30083. This can be optimally improved to 1, by choosing $x_1^{(2)} = 0.141784$.

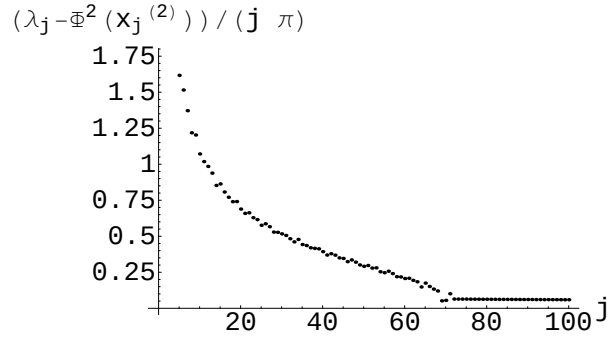

FIG. 9: The difference, divided by $j\pi$, of the j-th Riemann zero minus that value for the zero predicted from (3) using the *revised* set of turning points ($x_j^{(2)}$) (Fig. 7) and the *original* phases ($\alpha_k^{(1)}$) (Fig. 1)

$2.68927 \cdot 10^{-14}$ to 129157.) In Fig. 9, we show the differences (all positive) of the λ_j's minus their predicted values, divided by $j\pi$.

In this paper, we have *not* adhered to the apparent misstatement in [4, eq. (89)], that the Riemann zeros (λ_j) should be "properly normalized" ("unfolded" [18, eq. (6)]) as

$$\lambda_j \to \frac{\lambda_j}{2\pi} \log \lambda_j, \tag{9}$$

but rather conducted our analyses in terms of the "raw" unnormalized Riemann zeros themselves (λ_j's), similarly to the work of Wu and Sprung [5] (cf. [19]).

B. Non-iterative (simultaneous) approach

1. $n = m = 8$ *analyses*

We commenced an additional series of analyses — in lieu of the iterative scheme just proposed and discussed (but not fully pursued, due to apparent computational demands). For the case $n = m = 8$, we tried to *simultaneously* estimate the scaled phases (α_k) and turning points (x_j), *as well as* the frequency parameter γ (for a total of seventeen parameters). We sought to minimize — as we will throughout the remainder of this study — a certain sum-of-squares, one of the two addends being composed of the squared differences between the LHS and RHS of the (SUSY-QM) equations (3) and the other addend of the squared differences between the LHS and RHS of the (CBC) equations (5). (We simply, in effect, weighted the two sums *equally*, but there certainly appears — in retrospect — to be opportunity for refinement in the choice of weights, since the second (CBC) sum seemed to consistently contribute *considerably* more weight.) We also — as mentioned — allowed the parameter γ that determines the frequencies γ^k to vary (between 1 and 5), rather than holding it fixed at 3 (as we had preliminarily thought there was some numerical evidence for doing so earlier (sec. II)).

The minimum sum-of-squares we achieved was 181.6414. A predominant part of this sum — 130.236 — was attributable to the lack of fit to the CBC quantization conditions (5). *Remarkably*, all eight phases (α_k) were estimated to be essentially *zero* (or, effectively, the same 2π). The *largest* deviation of these eight estimates from 0 or 2π was, in fact, only $8.347 \cdot 10^{-8}$. (We had abandoned also here our earlier computational constraint that the phases be monotonically nondecreasing and only required, numerically, that they lie between 0 and 2π.) For γ we obtained an estimate of 1.4119. The eight estimated turning points (x_j) were (0.662734, 1.17022, 1.58516, 2.28689, 2.32938, 3.18343, 3.21295, 3.30561), which can be compared with (1.30083, 1.87866, 2.20626, 2.64243, 2.84142, 3.20489, 3.4613, 3.64459), based on the smooth Wu-Sprung potential (8). Based on these two sets of turning points — and $\alpha_k = 0$, $k = 1, \ldots, 8$ and $\gamma = 1.41119$ — the corresponding CBC ratios (in the same order of presentation) are (1.80006, 1.55891, 1.3248, 1.32142, 1.22064, 1.23564, 1.23128, 1.21166) and (1.46964, 1.34903, 1.19796, 1.26407, 1.14572, 1.23298, 1.201, 1.16905). We can see that the latter set of CBC ratios is clearly superior/more desirable — giving rise to a sum-of-squares

deviation of only 83.5937 *vs.* the 130.236 mentioned-before — but use of the original set of turning points ($x_j^{(1)}$) yields a much larger sum-of-squares for deviations from the other (SUSY-QM) set of equations (3) of 620.878, as opposed to the $51.4054 = 181.6414 - 130.236$ we obtained.

2. $n = m = 7$ analyses

We had also conducted some parallel $n = m = 7$ analyses. We obtained from Mathematica, three minima (with figures of merit of 69.6285, 140.887 and 171.939). The corresponding estimates of γ were 1.16585, 1.34436 and 1.4099. Of the 21 (7×3) phases estimated, none was greater than 0.000210 removed from either 0 or 2π.

We will find, apparently importantly, in Sec. V A that for this $n = m = 7$ case, we can obtain a much *improved* figure of merit of 13.703 by incorporating one additional parameter (σ) into the SUSY-QM model (3), one which *scales* the Weierstrass fractal function $W(x, \gamma, \frac{3}{2}, \alpha_k)$. Before doing so, however, we will examine, in detail, the fractal Wu-Sprung potential.

IV. ANALYSES OF THE WU-SPRUNG *FRACTAL* POTENTIAL

We implemented, for the case $n = 100$, with an algorithm provided by M. Trott, the *dressing transformation* for the *inversion* of the eigenvalues (λ_j's), employed by van Zyl and Hutchinson [9], in order to obtain the *fractal* form $V_{WS_{frac}}(x)$ of the Wu-Sprung potential (Fig. 10) (cf. [5, Fig. 2], [9, Figs. 1, 3]). In Fig. 11 we show the *non-smooth* component (the "residual" in statistical parlance) of the fractal WS potential. In other words, we have subtracted away from Fig 10, the smooth WS potential $V_{WS}(x)$. We have tried to manipulate the Weierstrass fractal function (2), as incorporated into (3) — assuming all $\alpha_k = 0$ — so as to closely resemble Fig. 11. A simply visual, non-rigorous analysis lead us to present Fig. 12, in which we take $\gamma = 2.3$ *and* multiply the Weierstrass fractal function term in (3) by 5 and subtract 10. (Possibly, the CM model might be modified, somewhat in line with this observation. So, it would appear, that even though the Weierstrass fractal function, with its fractal dimension D set to $\frac{3}{2}$ and the fractal component of the $V_{WS_{frac}}$ share the same fractal dimension, they seem to differ considerably in certain of their overall [scale,

location] properties. We will explore this issue in Sec. V.)

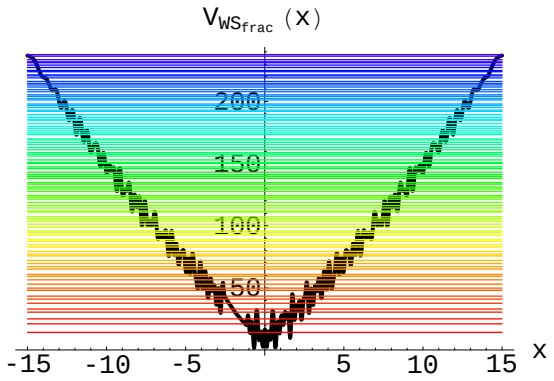

FIG. 10: *Fractal* Wu-Sprung potential, $V_{WS_{frac}}(x)$, based on the first 100 Riemann zeros

A. Turning points ($x_{j_h}^{frac}$) of the *fractal* Wu-Sprung potential

Using the results of the dressing transformation, we initially considered taking for the values of x_j^{frac}, those closest to the original smooth Wu-Sprung turning point ($x_j^{(1)}$), for which $\lambda_j = V_{WS_{frac}}(x_j^{frac})$, as our new/revised turning point to employ in the CM model.

Pertaining to the issue, for the edification of the reader, we will note that in an e-mail exchange of ours with M. Trott, he had commented: "But they (van Zyl and Hutchinson [9]) use an exact solution of the Schrödinger equation. So in their approach they never need turning points. This bring us back to my remark from the beginning of this project. What is a 'turning point' in a fractal potential? If you take the smallest x_{Min}, such that

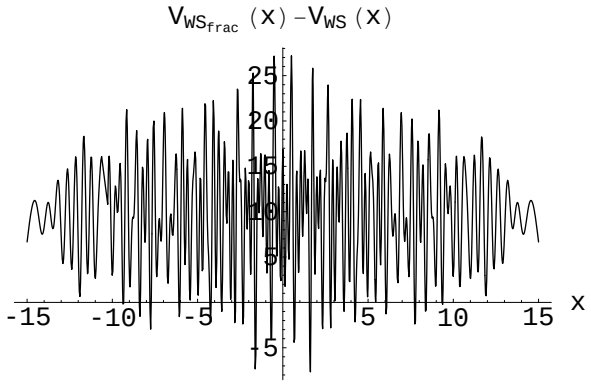

FIG. 11: *Non-smooth* component of the Wu-Sprung fractal potential $V_{WS_{frac}}(x)$, that is, $V_{WS_{frac}}(x) - V_{WS}(x)$.

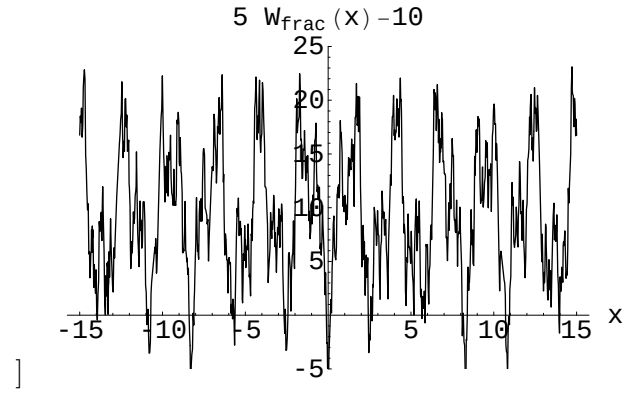

FIG. 12: Weierstrass fractal function contribution to (3) multiplied by 5, then diminished by 10, with $\gamma = 2.3$ and $\alpha_k = 0$, with intention of adjusting the Weierstrass fractal function to resemble Fig. 11 as closely as possible

$\int_{-x_{Min}}^{x_{Min}} \sqrt{e - V(x)} = n\hbar$ with $e = V(x_{Min})$, then, because of the fractal nature, the barrier could be very small and the tunnelling contributions from larger x could be quite significant." In response, Castro first wrote:" Since the Weierstrass function oscillates, there are many possible choices for the x_j^{frac}, so you have to choose for the turning points those which are the closest to the ones $[x_j^{(1)}]$ obtained from the smooth Wu and Sprung potential alone. This process will determine the x_j^{frac} points uniquely". Trott further suggested: "From an ordinary quantum mechanics point of view using the 'nearest' ones seems unconvincing to me. Already for the simple case of two wells separated by a wall, the classical JWKB formulas get nontrivial corrections" (cf. [20]). (However, in retrospect, it now appears that the most effective manner in which to resolve this issue — at least, in pragmatic terms — is to choose that x_j^{frac} for which the associated fractal CBC relation (5) is most closely satisfied.)

We, in fact, found *nine* possible values of $x_{1_h}^{frac}$, that is (0.0359371, 0.224349, 0.403363, 0.60336, 0.75138, 0.902281, 0.949646, 1.5688, 1.63925), satisfying the turning point relation $V_{WS_{frac}}(x_{1_h}^{frac}) = \lambda_1$. The correponding CBC ratios (Fig. 13) — (0., 0.766538, 1.04323, 0.871811, 1.42656, 1.26132, 1.30892, 1.09161, 1.27263) seemed, except obviously for the first, reasonably well-behaved. For the second Riemann zero (λ_2), the ten turning points found were (0.432856, 0.57922, 0.787248, 0.848629, 1.13689, 1.19066, 1.54042, 1.66097, 1.88178, 2.32703) with corresponding CBC ratios (Fig. 14) (0.966061, 0.848087, 1.2481, 1.18487, 1.24222, 1.26174, 1.14487, 1.35361, 1.24891, 1.16204). For λ_3, the sixteen turning

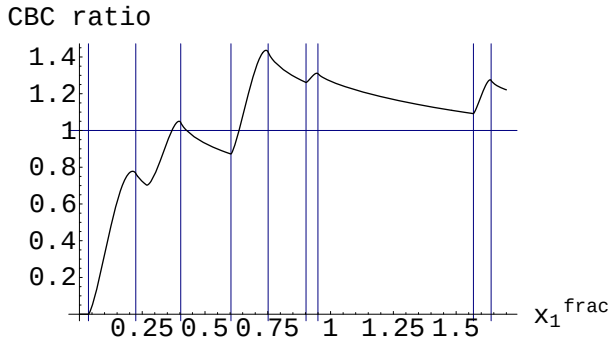

FIG. 13: CBC ratios based on the fractal Wu-Sprung potential $V_{WS_{frac}}(x)$. The nine ($h = 1, \ldots, 9$) turning points ($x_{1_h}^{frac}$) for which $V_{WS_{frac}}(x_{1_h}^{frac}) = \lambda_1$ are indicated.

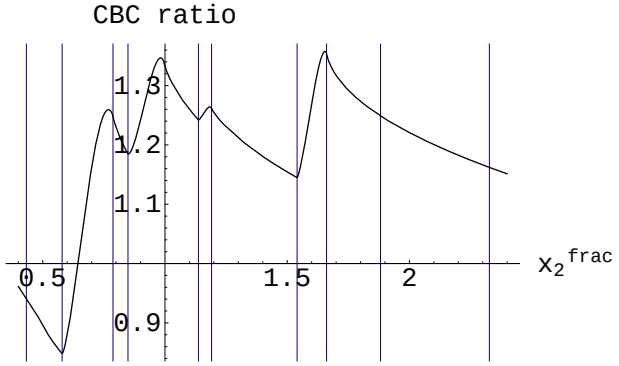

FIG. 14: CBC ratios based on the fractal Wu-Sprung potential $V_{WS_{frac}}(x)$. The ten ($h = 1, \ldots, 10$) turning points ($x_{2_h}^{frac}$) for which $V_{WS_{frac}}(x_{2_h}^{frac}) = \lambda_2$ are indicated.

points (0.450109, 0.563705, 0.816881, 1.0183, 1.10108, 1.22306, 1.38131, 1.39341, 1.5228, 1.67159, 1.86394, 1.90039, 1.90039, 2.30223, 2.35184, 2.79924) with corresponding CBC ratios (Fig. 15) of (0.765244, 0.689671, 1.01581, 1.15142, 1.09523, 1.15534, 1.08533, 1.08337, 1.04846, 1.22877, 1.14428, 1.15193, 1.15193, 1.07091, 1.0915, 1.02537). We also show results (Fig. 16) for $x_{50_h}^{frac}$, with turning points (9.11597, 9.22462, 9.4841, 9.9511, 10.019) and fractal CBC ratios (0.980756, 0.971956, 0.97427, 0.948974, 0.94763).

B. Formulas for certain fractal turning points

Continuing along these lines, we found that particular value (0.949646) of x for which $V_{WS_{frac}}(x) = \lambda_1$, and which, of the nine solutions, was, at the same time,

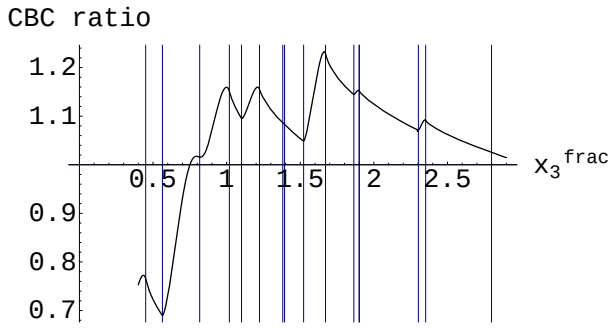

FIG. 15: CBC ratios based on the fractal Wu-Sprung potential $V_{WS_{frac}}(x)$. The sixteen ($h = 1, \ldots, 16$) turning points ($x_{3_h}^{frac}$) for which $V_{WS_{frac}}(x_{3_h}^{frac}) = \lambda_3$ are indicated.

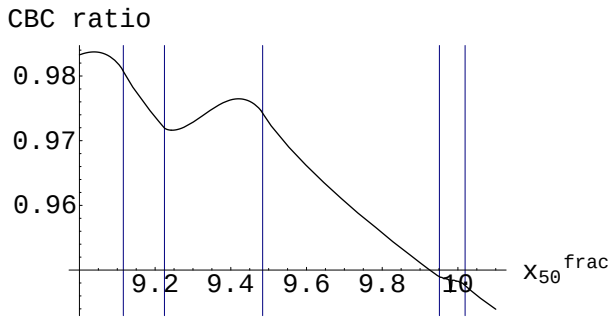

FIG. 16: CBC ratios based on the fractal Wu-Sprung potential $V_{WS_{frac}}(x)$. The five ($h = 1, \ldots, 5$) turning points ($x_{50_h}^{frac}$) for which $V_{WS_{frac}}(x_{50_h}^{frac}) = \lambda_3$ are indicated.

smaller than $x_1^{(1)} = 1.30083$, and *closest* to it. With the use of "Plouffe's inverter" (http://pi.lacim.uqam.ca/eng/), we obtained a remarkable formula that would appear to apply to it:

$$x_1^{frac} = 0.949646 \approx 0.99999996 \cdot 10^{-6} \frac{te^{\lambda_1}}{GS}, \tag{10}$$

where $t \approx 1.8392867$ is the *tribonacci constant* and GS is the *Gelfond-Schneider* constant, $2^{\sqrt{2}}$.

Proceeding further along these lines, the value ($x = 1.660974$) we obtained for x_2^{frac}, that satisfied $V_{WS_{frac}}(x) = \lambda_2$, and was smallest and closest to $x_2^{(1)} = 1.87866$ was expressible as

$$x_2^{frac} = 1.660974 \approx 1.0000028005 \cdot 10^{-21} \frac{e^{2\lambda_3}}{t \log^2(2 + \sqrt{3})}. \tag{11}$$

Additionally,

$$x_3^{frac} = 1.9003895 \approx 0.99999998 \cdot 10^{-40} e^{3\lambda_5} \frac{3Trott}{(2+\sqrt{3})^2}, \tag{12}$$

where $Trott = 0.010841015122311136$ is the *Trott constant*, and $x_3^{(1)} = 2.20626$. (The Trott constant has the property that it is invariant, in a certain sense. If one expands the number digit by digit as if it were a continued fraction, then the number remains the same [21].)

Further,

$$x_4^{frac} = 2.3843247 \approx 1.00000003037 \cdot 10^{-72} \frac{e^{4\lambda_7}}{t^2 Cahen^2 \log \zeta(5)}, \tag{13}$$

where $Cahen \approx 0.6434105462883$ is the *Cahen constant*, used in the theory of continued fractions. ($x_4^{(1)} = 2.64243$ and ζ is the Riemann zeta function — *exact* formulas for which are known for *even* integral arguments.)

Also,

$$x_5^{frac} = 2.8338417 \approx 1.00000004769 \cdot 10^{-106} \frac{\zeta(3) e^{4\sqrt{2}} e^{5\lambda_9}}{\Gamma(\frac{7}{12})}. \tag{14}$$

(x_5^{frac} is rather close to $x_5^{(1)} = 2.84142$. $\zeta(3)$ is known to be *irrational* and is sometimes referred to as "Apéry's constant" [22].)

V. *SCALING* THE WEIERSTRASS FRACTAL FUNCTION

The analyses underlying Figs. 11 and 12, and their comparison, indicated to us that possibly the CM model of the Riemann zeros might be enhanced by multiplying the Weierstrass fractal contribution (3) by some (new) scaling factor (σ). (Since in Sec. II, we were essentially finding parameters to set the Weierstrass function to zero, the issue of scaling was not germane there.) So, we modified the type of analyses reported in Secs. III B 1 and III B 2 to estimate σ, as well as the (scaled) phases (α_k), the turning points (x_j) and the frequency parameter (γ).

A. $n = m = 7$ analyses

We use exactly the same criterion of best (unscaled) fit, employed previously, that is the total sum-of-squares between the LHS's and RHS's of (3) and (5). The sum-of-squares we

obtained was 13.703 (8.48114 coming from the lack of fit to the CBC quantization conditions (5)), *much* superior to the best fit of 69.6285 in Sec. III B 2. This, of course, lends strong support for the relevance of incorporating the scaling parameter σ, which was set to 3.92036, along with $\gamma = 2.18081$ — *both* estimates being quite consistent with Fig. 12. The seven estimated phases were (0.915274, 6.28319, 6.28319, 1.20429, 5.33637, 0.700917, 0.0) — three of them being essentially 0 or $2\pi \approx 6.28318531$. The seven estimated turning points were (0.321253, 0.676572, 0.936234, 1.65921, 1.79613, 2.1688, 2.18378), considerably smaller than in Secs. III B 2 and III B 1. The associated CBC ratios — all now relatively close to unity — are (1.1386, 1.16732, 0.951104, 1.13392, 1.02881, 1.067, 1.06951).

At this stage, we could have continued this $n = m = 7$ analysis to see if we could obtain further minima with figures of merit less than 13.703. But now knowing that Mathematica could produce results for $n = m = 7$, we were interested in seeing how far we could "push" Mathematica for cases $n = m > 7$. So, rather than now dwelling on a particular $n = m$ case, we kept seeking higher-order instances. (At this point, we treated each analysis independently, that is we did not employ results of earlier [lower-dimensional] analyses as initial guesses.) We did obtain single minima for $n = m = 8$ and $n = m = 9$, but the figures of merit were rather weak (39.1008 and 85.689), so we do not detail the results here.

B. $n = m = 10$ analyses

Now we expand to the case of ten phases and ten turning points. The (relatively quite *excellent*) sum-of-squares we obtained was 2.86609 (2.68872 coming from the lack of fit to the CBC quantization conditions (5)). The estimate of γ was 1.30466 and of σ, 1.49575. The ten estimated phases were (6.28319, 6.28319, 1.27142, 0.0493542, 6.28319, 0.0555025, 0.0000178313, 6.28319, 0., $6.00153 \cdot 10^{-23}$), *most* of them being essentially 0 or $2\pi \approx 6.28318531$. The ten estimated turning points were (0.38402, 0.665384, 0.915631, 1.32033, 1.42245, 1.83676, 1.95767, 2.33568, 2.68742, 3.06041), considerably smaller than in Secs. III B 2 and III B 1, where the scaling parameter (σ) was absent. The associated CBC ratios — most now relatively close to unity — are (1.27306, 1.142, 1.00359, 1.03838, 0.969627, 1.02007, 1.0058, 0.978438, 1.00323, 0.984601).

So, an important unresolved question is whether or not ideally *all* the phases (α_k) should be set to zero, or whether the fact that all the phases were estimated as zero in Sec. III B 1

was principally a manifestation of the need for a scaling parameter *greater* than unity. This is because if one sets all the phases to zero, the term-by-term interference in the Weierstrass fractal function is minimized and its overall contribution/influence/magnitude increased. (I thank Carlos Castro for this last observation.)

1. Zero phases

To address this last-discussed issue, still within the $n = m = 10$ scenario, we *a priori* set all ten phases (α_k) to zero, leaving us with twelve parameters (ten turning points, plus γ and σ) to estimate. We obtained four minima, one relatively inferior (24.0743) and three, all yielding approximately 7.2358 (6.758 of this from the CBC equations) — but all more than the 2.86609 obtained immediately above — for the sum-of-squares, and all with essentially the same set of estimates. The estimates were $\gamma = 1.25274$, $\sigma = 1.23289$ (both interestingly close to one another) and for the turning points (0.406011, 0.72083, 0.88735, 1.21503, 1.38215, 1.72066, 2.07865, 2.24067, 2.81678, 2.91862). The CBC ratios were (1.4716, 1.20207, 1.04624, 1.0322, 0.953197, 0.985181, 0.987027, 0.9602, 1.03323, 0.995425).

So, no yet fully convincing evidence for the proposition that *all* the phases (α_k) should be set to zero, has appeared in this $n = m = 10$ suite of analyses (though Castro believes this is an interesting hypothesis well worth pursuing).

C. $n = m = 12$

We were able to obtain two minima (*independently*-generated with different random seeds) for this case, having associated sums-of-squares of 4.7436 (4.51953 attributable to the fit to the CBC quantization conditions) and 4.88101 (4.59739 so-attributable).

These two minima had rather similiar estimates of γ, σ, as well as of the twelve turning points. (For the smaller of the two, γ and σ were estimated as 1.16902 and 1.90025, and for the larer, 1.17209 and 1.79825.) The turning points for the smaller (of the two small) minima were: (0.370638, 0.518695, 0.65557, 1.3734, 1.49501, 1.90065, 2.13024, 2.25476, 2.83058, 2.96561, 3.18434, 3.69962), and for the larger of the two (0.371207, 0.526829, 0.697696, 1.33586, 1.45628, 1.91474, 2.13455, 2.25897, 2.76173, 2.88164, 3.10636, 3.50429). The phases ($2\pi\alpha_k$) for the smaller of the two were: (5.06388, 1.19176, 5.10283, 5.10239, 1.54197, 4.87505,

5.75582, 5.07329, 6.28319, 6.28319, 0.491806, 0.) (three being essentially 0 or 2π) and (1.36199, 6.28319, 5.32029, 3.14014, 6.28319, 0.932408, 1.48183, 6.2407, 0.811536, 6.28186, 0.0160344, 0.) (five now being essentially or quite close to 0 or 2π). The CBC ratios based on the smallest (of the three $n = m = 10$) minima were: (1.45746, 1.09132, 0.891351, 1.03399, 0.967626, 1.0088, 1.01311, 0.981312, 1.01104, 0.986514, 1.00474, 1.00054).

D. $n = m = 15$

Mathematica yielded a minimum having a sum-of-squares of 10.8781, 10.1905 of the total stemming from deviations from the idealized CBC relationships.

The estimate of γ was 1.10999 and of the scaling parameter σ, 2.39239. The fifteen phases were estimated to be (5.85115, 1.90972, 6.07707, 3.38707, 5.79917, 3.01828, 5.21112, 0.972974, 6.28319, 4.06528, 5.13804, 1.09178, 5.42993, 0.0000400221, 0.887475) and the fifteen turning points, (0.427238, 0.575873, 0.674962, 0.964599, 1.67025, 1.86543, 1.99707, 2.09904, 2.87102, 2.96694, 3.12156, 3.26476, 3.37853, 3.42232, 3.66246). The resultant CBC ratios were (1.62295, 1.205, 0.970261, 0.919054, 0.964421, 1.03902, 1.01992, 0.974149, 1.00741, 0.984101, 1.00373, 1.01898, 1.01317, 0.977452, 0.996592).

Subsequently, we obtained a second minimum (starting with different random seeds), with a slightly inferior sum-of-squares of 11.6345 (10.9979 due to failure to completely satisfy the CBC relations). The estimate (1.10638) of γ obtained was notably similar to the first estimate (1.10999), while the estimate of σ was 1.92895 *vs.* 2.39239, previously. The estimated phases were (1.44074, 6.28318, 1.66813, 0.542437, 2.10471, 4.76708, 2.12488, 0.0381873, 1.27475, 0.672527, 1.10953, 1.92716, 5.96083, 0.00013761, 0.) and the estimated turning points, (0.447782, 0.605638, 0.711853, 1.03604, 1.65431, 1.87966, 2.02289, 2.13206, 2.85323, 2.95601, 3.11569, 3.25825, 3.37216, 3.41606, 3.70782). The *correlation coefficient* between the two sets of turning points was extremely high, 0.999796, while that between the two sets of phases was positive, but apparently quite weak, 0.174294. (The sets of turning points are constrained to be strictly increasing, while the phases are not.) This can be (maximally) improved to 0.471313 by adding $\theta = \pi$ to the second set of phases (Fig. 17). The correlation between the two sets of CBC ratios was extremely high, 0.997186. (Obviously, no ordering constraints has been placed upon them.)

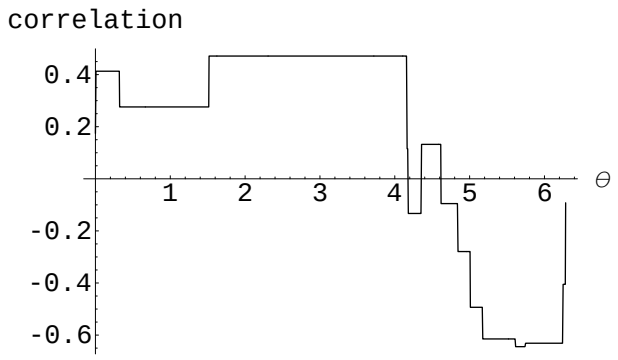

FIG. 17: Correlation coefficients between the first set of phases for the $n = m = 15$ case, and the second set of phases, with the addition to its members of an angle $\theta \in [0, 2\pi]$. The highest plateau of level 0.471313 extends from $\theta = 1.56108995$ to 4.1583035

E. $n = m = 20$

Initially, we obtained a minimum with a somewhat disappointingly large (in comparison with previous analyses) sum-of-squares of 60.1355 (57.0834 stemming from the failure to fully satisfy the CBC relations). The estimate of γ was 1.03784. Then, we obtained a somewhat superior sum-of-squares of 53.6492 (50.1484 coming from the lack of complete fit to the CBC relations). The estimate of γ, 1.049, was quite similar.

Ultimately though, we found a much superior solution with a sum-of-squares equal to 11.4018, of which 10.3952 was attributable to the failure to fully fit the CBC relations. The estimate of γ was 1.08285 and of σ, 1.23124. The twenty phases were (6.28319, 5.12918, 1.82172, 0.627236, 2.28354, 6.28057, 2.09377, 2.27574, 6.28319, 6.28319, 1.39899, 1.05003, 4.08259, 0.00871371, 6.28319, 5.20743, 0.00527643, 6.28319, $3.08389 \cdot 10^{-7}$, 0.00224054) — half of them being quite proximate to 0 or 2π — and the twenty turning points, (0.430261, 0.581042, 0.682297, 0.990577, 1.66733, 1.8869, 2.03975, 2.16318, 2.7836, 2.8999, 3.11796, 3.36483, 3.61917, 3.71294, 4.1214, 4.23216, 4.39019, 4.59062, 5.39774, 5.49934). (Possibly, the relatively large number of phases near either 0 or 2π is a computational artifact, since these are the *extreme* values between which the phases are constrained to lie.) Additionally, the resultant CBC ratios were (1.63002, 1.21105, 0.97568, 0.925948, 0.959536, 1.03755, 1.02111, 0.978159, 1.01279, 0.983753, 0.998834, 1.01199, 1.00774, 0.97948, 1.01524, 1.00143, 0.997587, 0.993286, 1.00448, 0.994628).

We have been investigating the $n = m = 25$ case (both with unconstrained phases and

phases set to zero) — with some programming improvements provided by M. Trott — but do not have any specific results to report presently. (It appears that several days on a PowerMac are required to locate a single relative minimum.)

1. Decreasing trend in estimates of γ

We see an undeniable trend in the several analyses above. As the number of unknowns $(n + m + 2)$ increases, the parameter γ *decreases*, possibly indicative of a convergence to its theoretical lower bound for the Weierstrass fractal function of 1. (For $n = m = 7$, our one estimate of γ was 2.18081; for $n = m = 10$, the estimate was 1.30466; for $n = m = 12$, we had two estimates of 1.16902 and 1.17209; for $n = m = 15$, 1.10999 and 1.10638; and for $n = m = 20$, 1.03784, 1.049 and 1.08285.) Szulga and Molz have shown that in the limit $\gamma \to 1$ (with random phases, in the case $D = \frac{3}{2}$ before us here), "the Mandelbrot-Weierstrass process is a complex fractional Brownian motion" [23] (cf. [24, 25, 26, 27]). In the Castro-Mahecha model, one takes the *real* part of the Mandelbrot-Weierstrass function (which CM term the Weierstrass function). To statistically test whether or not the estimated series of phases we obtain is *random* in nature, one can apply "Rao's spacing test" [28]. (Also, the Rayleigh test and the Kuiper's V test are sometimes employed.) Applying this test to the first two sets of twenty phases reported for our $n = m = 20$ analyses in Sec. V E, we obtained statistics of 192.199 and 158.86, respectively. Any result greater than 192.17 is statistically significant at the $p = 0.001$ level of probability, and any result greater than 154.31, at the $p = 0.10$ level [28, Table II]. There is, thus, rather strong evidence that the hypothesis that the phases are random should be *rejected*.

VI. DISCUSSION

On the scientifically important question of possible *falsifiability*, the Castro-Mahecha supersymmetric model of the nontrivial Riemann zeros — and that of Wu and Sprung [5] — would *fail* (as Carlos Castro indicated) if it could be demonstrated that the shape of the potential were *multifractal*, so that the fractal dimension would no longer be a *constant* ($D = \frac{3}{2}$). We are not cognizant of any evidence of this, though. However, it might be of some value to formally test for such a possibility. (Though we are aware of no multifractal counterpart

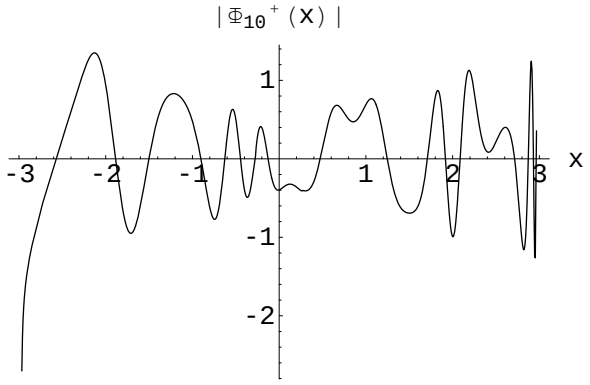

FIG. 18: Absolute value ($|\Phi_{10}^{+}(x)|$) of the wavefunction corresponding to the tenth eigenvalue λ_{10} and the tenth turning point $x_{10} = 2.96694$ reported for the $n = m = 15$ analysis (smaller of the two minima) in Sec. V D

to the Weierstrass function, Castro suggested that one could sum (or possibly integrate) over the fractal dimension (D).) Additionally, still within a "unifractal" framework, Castro put forth the idea of integrating (thus, generalizing) the Weierstrass fractal function — with fractal dimension D held constant at $\frac{3}{2}$ — over the parameter γ, using some appropriate weighting function $f(\gamma)$.

The presumptive Hilbert-Polya operator would have eigenvalues equal to the λ_j's. It might be of interest to attempt to estimate its eigen*functions* within the same postulated quasi-classical (CBC) framework employed in the CM model, and in our analyses above. In Sec. 6.3 of [29] (also [11, eq. (56)]) there are presented formulas for the quasi-classical wave functions. The appropriate fractal extensions of these formulas — following the *ansatz* employed in (5) — would need to be employed (cf. [30]). An initial effort of ours along these lines — by simple way of a single illustration — yielded Fig. 18. In the context of their foundational article [5, p. 2597] (cf. [31]), "Riemann zeros and a fractal potential", Wu and Sprung noted that "All the wave functions decay exponentially beyond the turning point, and thus quickly die away. This implies that the lower energy levels have very small influence on the potential beyong their turning points ... Clearly, the potential in the low energy range has greater 'responsibility' than that in a higher energy range, thus it has more structure ... Based on this argument, the finest structure will be determined by the wave number of the last wave function."

It would be of interest to estimate *all* the n wavefunctions in our various $n = m$ analyses

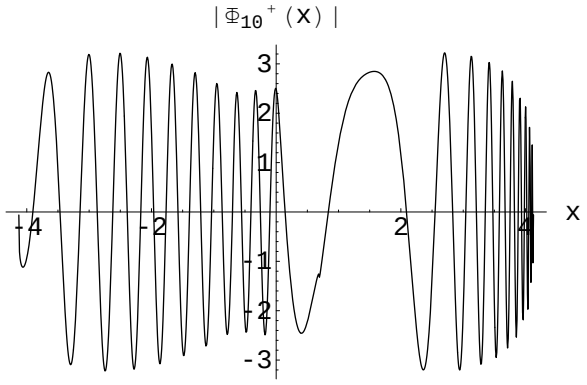

FIG. 19: Counterpart to Fig. 18 based simply on the *smooth* Wu-Sprung potential, *without* any fractal contribution, and original (non-fractal) formulas for the quasi-classical eigenfunctions

above, and examine whether or not the fractal SUSY Schrödinger equation (6) is (at least, approximately) satisfied. This would be, in some sense, a test of the appropriateness of the fractal extension of the CBC relations postulated by Castro and Mahecha (adopted by them in order to avoid having to directly solve (6)). (It would also, of course, be of interest to attempt to solve (6) more directly, rather than having to resort to the fractal CBC *ansatz* of CM.)

In Fig. 19 we show the counterpart to Fig. 18 based simply on the *smooth* Wu-Sprung potential, without any fractal contribution, and original (non-fractal) formulas ([29, eq. (6.40)], [11, eq. (56)]) for the quasi-classical eigenfunctions. It would be an interesting exercise to further duplicate some of the analyses conducted here, but with the replacement of the fractal CBC equations (5) with the (conventional) CBC equations.

Throughout the minimization analyses above, for the sake of simplicity (and to avoid the possible confusion of issues), we have relied upon a quite elementary least-squares fitting. Modifying this approach to give more equable weighting to the two sets of coupled equations, and perhaps to lower and higher Riemann zeros and turning points might prove useful.

CM believed "that their fractal SUSY QM model, once the optimum value for the amplitude factor γ is known, has a great chance of truly reproducing the zeta zeros, and proving the [Riemann Hypothesis], by simply establishing a one-to-one correspondence among the values of the infinite phases of our Weierstrass function with the zeta zeros" [4, sec. 6]. We have tried to make a contribution in such a direction here.

Castro suggested that the most salient/interesting aspect of our several analyses above

had emerged in Sec. V B 1, where for the case $n = m = 10$ we had *set* the ten phases to zero (doing so which had been strongly suggested by the results of the immediately preceding analysis in which the phases were *not* constrained, and allowed to vary between 0 and 2π, but found, *nevertheless*, to be predominantly 0 or 2π). The estimates of the frequency parameter γ and the scaling parameter σ were quite intriguingly close (1.25274 and 1.23289). However, the figure of merit, 7.2358, in this zero-phase analysis was somewhat inferior to that [2.86609] in that unconstrained $n = m = 10$ analysis, which rather induced us here not to subsequently pursue solely further analyses ($n = m > 10$) in which the phases had been *a priori* set to zero — but rather let them freely vary. Also, we suspected, as previously mentioned, that the predominance of 0's or 2π's might be, in some way, a computational artifact, since these are the imposed limits on the phases. (The minimization procedure, we speculated, might drive the phases to these end points, beyond which it could not further proceed to seek improvements, and would therefore *terminate* there. Castro suggested that setting the range of possible phases to be $[-\pi, \pi]$ would obviate this particular problem — but possibly introduce new ones. We intend to investigate such a direction.)

Perhaps somewhat relatedly, as one of their "spectral speculations", Berry and Keating [32, p. 260] remarked that the "Maslov phases associated with the [classical periodic orbits of the Riemann dynamics] are also peculiar: they are all π. The result appears paradoxical in view of the relations between these phases and the winding numbers of the stable and unstable manifolds associated with periodic orbits , but finds an explanation in a scheme of Connes". (The Maslov phases appear when one modifies the Bohr-Sommerfield quantization rules by equating the WKB integrals (orbits) to $j\pi$ plus a Maslov phase factor, instead of $j\pi$.)

Castro suggested that the possibility the Weierstrass fractal function might assume the form of classical Brownian motion was an unappealing one, seeing that this would apparently imply that the phases (α_k) must be random. (In Sec. V E 1 we deduced certain statistical evidence that the estimated phases [allowed to freely vary] were *not*, in fact, random. Of course, we know this to be strictly true, since the phases are constructed by our estimation procedure.)

Appendix

At our suggestion, D. Dominici investigated the problem of inverting the Wu-Sprung potential (1) [5, eq. (7)]. His analyses have been presented in a "preliminary report" [14].

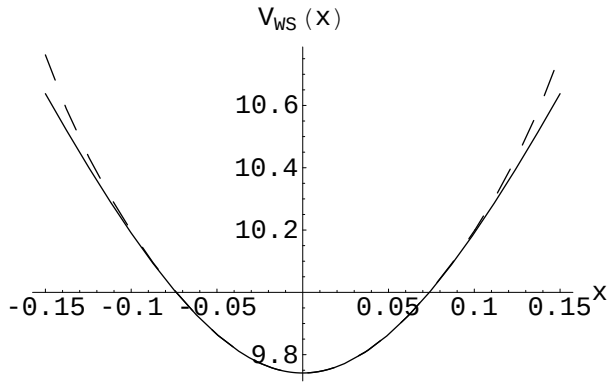

FIG. 20: Inverted smooth Wu-Sprung potential (1) — using the Mathematica Interpolation command on a data table of resolution $\frac{1}{40}$ — and the approximation (dashed lines) to the inverted potential using the first three terms (17) of the Dominici series expansion (15)

Dominici gives explicitly the first *ten* coefficients (a_k) of a power series expansion,

$$V_{WS}(x) = V_0 + \Sigma_{k=1}^{\infty} a_k (\pi x)^{2k} \omega^{2k-1} (-V_0)^{1-k}, \tag{15}$$

where

$$\omega = \Big[\ln \Big(\frac{V_0}{2\pi} \Big) \Big]^{-1}. \tag{16}$$

(For the critical value $V_0 = 2\pi$, above which $V_{WS}(x)$ is *single*-valued, the expansion (15) is no longer valid. A separate analysis [14, Sec. 2.2] is, then, of interest.) Using just the first three of these coefficients,

$$a_1 = \omega; a_2 = \frac{4}{3}\omega^2; a_3 = \frac{8}{15}\omega^2 + \frac{28}{9}\omega^3, \tag{17}$$

we obtain Fig. 20.

In the analyses reported in the body of this paper, we had relied upon the Interpolation command of Mathematica for the purpose of inversion, but we anticipate employing the results of Dominici [14] in our further work. C. Krattenthaler has indicated that for the purpose of studying the *asymptotic* behavior of the coefficients of the power series, it would be best to employ the methodology of Lagrange inversion.

Acknowledgments

Carlos Castro kindly introduced me to his joint work [4] with Jorge Mahecha, proposed avenues of research to pursue, and discussed in great detail the analytical developments.

Further, I would like to express gratitude to the Kavli Institute for Theoretical Physics (KITP) for computational support, to Michael Trott of Wolfram Research Inc. for his more than generous assistance and expertise in terms of Mathematica computations, as well as for his critical interest and comments, and to Diego Dominici for his interest in the problem of inverting the Wu-Sprung potential [14].

---

[1] J. B. Conrey, Notices Amer. Math. Soc. **50**, 341 (2003).

[2] L. A. Bunimovich and C. P. Dettmann, Phys. Rev. Lett. **94**, 100201 (2005).

[3] D. Rockmore, *Stalking the Riemann Hypothesis* (Pantheon, New York, 2005).

[4] C. Castro and J. Mahecha, Int. J. Geom. Meth. Mod. Phys. **1**, 751 (2004).

[5] H. Wu and W. L. Sprung, Phys. Rev. E **48**, 2595 (1993).

[6] M. V. Berry and Z. V. Lewis, Proc. Roy. Soc. London **370**, 459 (1980).

[7] N. N. Khuri, Math. Phys. Anal. Geom. **5**, 1 (2002).

[8] H. C. Rosu, Mod. Phys. Lett. A **18**, 1205 (2003).

[9] B. P. van Zyl and D. A. W. Hutchinson, Phys. Rev. E **67**, 066211 (2003).

[10] N. Laskin, Phys. Rev. E **66**, 056108 (2002).

[11] A. Inomata and G. Junker, Phys. Rev. A **50**, 3638 (1994).

[12] H. M. Edwards, *Riemann's zeta function* (Academic Press, New York, 1974).

[13] C. Ma and Y. Hori, in *ASME 2003 Design Engineering Technical Conferences* (2003), (DET2003VIB-48736).

[14] D. Dominici, math.CA/0510341.

[15] R. K. Bhaduri, J. Sakhr, D. W. L. Sprung, R. Dutt, and A. Suzuki, J. Phys. A **38**, L183 (2005).

[16] M. Planat and H. C. Rosu, Phys. Lett. A **315**, 1 (2003).

[17] L. Rüschendorf, Ann. Statist. **23**, 1160 (1995).

[18] N. M. Katz and P. Sarnak, Bull. Amer. Math. Soc. **36**, 1 (1999).

[19] H. Wu, M. Valliéres, D. H. Feng, and D. W. L. Sprung, Phys. Rev. A **42**, 1027 (1990).

[20] M. Robnik, L. Salasnich, and M. Vraničar, Nonlin. Phen. Complex Syst. **2**, 49 (1999).

[21] S. R. Finch, *Mathematical Constants* (Cambridge U. P., Cambridge, 2003).

[22] R. Apéry, Astérique **61**, 11 (1979).

[23] J. Szulga and F. Molz, J. Statist. Phys. **104**, 1317 (2001).

[24] J. Szulga, Statist. Prob. Lett. **56**, 301 (2002).

[25] V. Pipiras and M. S. Taqqu, Fractals **8**, 369 (2000).

[26] P. K. Rawlings, J. Statist. Phys. **111**, 769 (2003).

[27] P. Biane, J. Pitman, and M. Yor, Bull. Amer. Math. Soc. **38**, 435 (2001).

[28] G. S. Russell and D. J. Levitin, Commun. Statist.: Simul. Comput. **24**, 879 (1995).

[29] G. Junker, *Supersymmetric Methods in Quantum and Statistical Physics* (Springer-Verlag, Berlin, 1996).

[30] D. Wójcik, I. Białynicki, and K. Życzkowski, Phys. Rev. Lett. **85**, 5022 (2000).

[31] M. Tomiya and S. Sakamoto, e-J. Surf. Sci. Nanotech. **1**, 175 (2003).

[32] M. V. Berry and J. P. Keating, SIAM Review **41**, 236 (1999).

[33] M. Trott suggested — in analogy to the self-consistent solution of Schrödinger and Poisson equations for some charged system — that it might be a more superior/stable iterative scheme, to at each stage *combine* the current, revised estimates of the $\alpha_k^{(i)}$'s and $x_j^{(i)}$'s with those from the preceding step of the iterative procedure, in fact, perhaps much more strongly weighting the preceding $(i-1)$ estimates. We have not yet thoroughly pursued this possibility, though.